Ring Currents and Magnetic Properties of *s*-Indacene, an Archetypal Paratropic, Non-Antiaromatic Molecule

R. Soriano Jartín, A. Ligabue, A. Soncini, and P. Lazzeretti*

Dipartimento di Chimica, Università degli Studi di Modena e Reggio Emilia, via G. Campi 183, 41100 Modena, Italy

Received: June 18, 2002; In Final Form: September 17, 2002

Magnetic susceptibility and nuclear magnetic shielding at the nuclei of *s*-indacene have been evaluated by a series of different approximations and a large Gaussian basis set. An ab initio model of magnetic field induced current density was developed, showing that intense paramagnetic flow takes place within the π electrons. It causes strong upfield chemical shift of protons attached to hexagonal and pentagonal rings. The magnetic susceptibility tensor is typical of a diamagnetic molecule but is characterized by small anisotropy. Group-theoretical methods developed by Steiner and Fowler indicate that *s*-indacene can be classified as a 2p + 4d system, in which the paramagnetic circulation of two electrons in the highest occupied orbital of B_g symmetry overwhelms the diamagnetic flow of four electrons in occupied A_u orbitals. Because of its unique structural and magnetic properties, *s*-indacene can be described as a limit system between the classes of aromatic and antiaromatic molecules.

1. Introduction

Attempts at connecting the aromatic properties of conjugated planar cyclic molecules with their peculiar response to magnetic perturbations have long been made. The relevant literature has been reviewed in articles recently appeared.[1−12]

There is large experimental evidence documenting that the out-of-plane component of the susceptibility tensor of unsaturated benzenoid hydrocarbons with $(4n + 2)$ delocalized π electrons is significantly larger than that of corresponding saturated systems. The magnetic anisotropy of these molecules is much stronger than that in corresponding saturated compounds. This typical behavior is unanimously ascribed to the special mobility of a delocalized electron cloud in the presence of magnetic field and to its ability to sustain intense diamagnetic ring currents, which are also responsible for proton downfield shift in nuclear magnetic resonance spectra of aromatic species. Thus, NMR spectroscopy provides the tools to "measure aromaticity".[13]

Because unambiguous definitions of aromatic character have been a matter of major concern for chemists,[14] the enhanced diamagnetism of conjugated planar cyclic systems has been advocated as its fingerprint. Accordingly, "diatropicity" and "aromaticity" are commonly considered as synonyms. Relying on a symmetrical argument, it has been suggested by many authors that "paratropicity" implies "antiaromaticity".[15−18]

Berthier, Mayot, and Pullman[19] have first shown that positive contributions from π electrons to the magnetic susceptibility of molecules such as pentalene and heptalene are expected by a straightforward application of the London theory.[20] Apparently, in these molecules, a magnetic field perpendicular to the molecular skeleton induces paramagnetic ring currents in the π cloud.[21]

A theoretical treatment of monocyclic conjugated polyenes with $4n$ π electrons was reported by Pople and Untch at semiempirical level of accuracy, showing evidence for the existence of magnetic field induced paramagnetic ring currents, which cause upfield (downfield) chemical shift for protons outside (inside) the ring.[22] The Pople model was successfully applied to interpret the ring current effects observed by Sondheimer in annulenes.[23]

2. Mixed Aromatic and Antiaromatic Properties of *s*-Indacene

s-Indacene is an elusive molecule and decomposes very rapidly because of its extreme reactivity.[24] However, its substituted derivatives are known; for instance, 1,3,5,7-tetra-*ter*-butyl-*s*-indacene has been synthesized and its X-ray structure has been reported,[25,26] showing evidence for D_{2h} symmetry of the 12-carbon cyclic arrangement. The low-temperature ^{13}C NMR spectrum contains only four different peaks corresponding to the magnetically inequivalent carbon atoms of its skeleton.[25] Unless this pattern is due to packed structure of the molecules within the crystal phase, this should provide a further piece of evidence in favor of D_{2h} geometry. Relying on the Hückel approximation, Heilbronner and Yang[27,28] gave a qualitative interpretation of the mechanism whereby the substituents lead to a stabilization of the polyenic cycle and to delocalization of π electrons, driving the carbon ring to D_{2h} structure.

At any rate, the parent molecule *s*-indacene is a 12 π electron system, formally antiaromatic according to the Hückel $(4n + 2)$ rule. Semiempirical studies indicate that the C_{2h} structure **1** is more stable than that with delocalized D_{2h} symmetry **2**.[25,27,29]

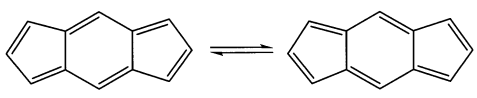

1

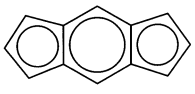

2

10.1021/jp0263267 CCC: $22.00 © 2002 American Chemical Society
Published on Web 11/08/2002

Two energy-degenerate valence isomers **1** with localized double bonds should exist. Ab initio calculations at Hartree−Fock level of accuracy validate this hypothesis, predicting an energy stabilization as large as ∼5.1 kcal mol^{-1},[30] which favors form **1** over **2**.

On the other hand, high-level quantum mechanical approaches, employing complete active space self-consistent field second-order many-body perturbation theory (CASPT2), suggest that the D_{2h} structure of *s*-indacene is ∼3.1 kcal mol^{-1} more stable than the alternative C_{2h} form.[31] Geometrical parameters calculated by density functional theory, within the local density approximation (LDA) and higher Becke−Perdew (BP) corrections, are very close to those yielded by the ab initio methods and are in excellent agreement with experimental data available for 1,3,5,7-tetra-*tert*-butyl-*s*-indacene.[31]

However, according to other authors, the *s*-indacene puzzle is still open,[32] as no convincing evidence has so far been reported via theoretical calculations of molecular energies.[30,31,33] Three sets of criteria for aromaticity were taken into account in ref 32, based on geometry, magnetic properties, and stability. The results are quite in conflict into one another: the calculated Julg parameter (ranging from 0 for a hypothetical fully localized alternant six-membered ring to 1 for benzene) is 0.920 for **1** and 0.970 for **2**, compared with 0.90 for anthracene, implying aromaticity in the opinion of the authors.[32]

The aromatic stabilization energy (ASE) estimated for **1** is 10.8 kcal mol^{-1}, whereas that of anthracene, 61.8 kcal mol^{-1}, is approximately 6 times larger. The nucleus-independent chemical shift (NICS)[34] values calculated for the C_{2h} structure are +21.6 and +17.7, respectively, for the five-membered and six-membered rings, while the corresponding results for the D_{2h} structure are +25.8 and 20.8.[32] Therefore, allowing for these results, the *s*-indacene molecule should be regarded as having mixed aromatic and antiaromatic character.[18]

However, many questions are still open. For *s*-indacene, no information is available on the aromatic ring current shieldings (ARCS) introduced by Jusélius and Sundholm.[35] These authors studied aromatic, antiaromatic, and nonaromatic dehydroannulenes and found that bond-length alternation is smaller for antiaromatic than for the nonaromatic molecules.[36] Thus bond-length alternation would not necessarily provide a good measure of the degree of aromatic−antiaromatic character. These findings seem to imply that the Julg measure cannot be applied on antiaromatic molecules.

3. Theoretical Magnetic Properties of *s*-Indacene

The present study stems from the evident failure of previous attempts at fully characterizing *s*-indacene via commonly used aromaticity indicators. Its aim is that of considering objective physical criteria based on (i) ab initio models of the ring currents induced by a magnetic field perpendicular to the molecular plane and (ii) accurate estimates for magnetic properties.

The molecular geometry of *s*-indacene $C_{12}H_8$ has been optimized via the Gaussian program[37] at the B3LYP level of approximation using the 6-31G** and the 6-311G** basis sets. The structural parameters obtained from the two basis sets are very close to one another. The optimum geometry corresponds to the C_{2h} symmetry **1** with two planar valence isomers. Attempts at optimizing the molecular structure with the constraint of D_{2h} symmetry, corresponding to the delocalized form **2** (see Table 1 for carbon−carbon computed bond lengths), yielded one imaginary frequency value. Thus, the calculations of magnetic properties and grids of current density field were carried out via the SYSMO code[38] retaining the 6-31G** C_{2h} structure.

TABLE 1: Carbon−Carbon Distances (Å)

	6-31G**		6-311G**	
	C_{2h}	D_{2h}	C_{2h}	D_{2h}
C12−C1	1.383	1.406	1.379	1.404
C1−C3	1.445	1.423	1.445	1.422
C3−C8	1.452	1.447	1.450	1.445
C3−C5	1.380	1.399	1.377	1.397
C5−C7	1.419		1.418	
C7−C9	1.399		1.396	
C9−C11	1.432		1.432	

At any rate, according to our experience, small changes in geometrical parameters do not introduce major alterations of the current density pattern. Therefore, the conclusions obtained here are not expected to vary significantly if molecular geometry is slightly changed.

Several basis sets of increasing size and quality were tested until a good degree of convergence was found for theoretical predictions of magnetic properties. The best results arrived at in this study have been reported in Tables 2−6. The largest basis set consists of 676 contracted Gaussians. It has been constructed using the (11s/7p) substratum from the van Duijneveldt's compilation[39] enriched by four sets of 3d Gaussians functions on carbon with exponents 1.61, 0.43, 0.15, and 0.062 and one set of 2p functions on H with exponent 0.54. The contraction scheme is (11s7p4d/7s1p) → [6s7p4d/5s1p].

Calculations of magnetic properties were also carried out via the DALTON code[40] using the same basis set with London phase factors, that is, 676 gauge-including atomic orbitals[41] (GIAO) basis sets, also referred to as London orbitals (LO), which guarantee translational invariance and faster convergence to the Hartree−Fock limit.

A number of approximated computational schemes relying on gaugeless basis sets were tested at the Hartree−Fock level of accuracy, namely, the conventional common origin (CO) approach, and four numerical techniques based on continuous transformation of the origin of the currents density (CTOCD), formally annihilating diamagnetic (DZ) or paramagnetic (PZ) contributions. DZ2 and PZ2 variants employ damping factors to improve the accuracy of computed magnetic shielding. The underlying theory is available from refs 2 and 42−44 in which the notation retained here is described. The CTOCD-DZ and CTOCD-PZ values for magnetic susceptibility and nuclear magnetic shieldings are invariant in a gauge translation.

Theoretical predictions for magnetic susceptibility components are shown in Table 2. According to our numerical test, the case of *s*-indacene is quite critical and requires big computer effort. Total values of $\chi_{\alpha\beta}$, reported with five significant figures, are the difference of big diamagnetic and paramagnetic contributions that are 1 or 2 orders of magnitude larger. Spurious cancellation of errors was found to occur when basis sets of reduced size are adopted.

Conventional common origin values are partitioned into diamagnetic, χ^d, and paramagnetic, χ^p, contributions evaluated with respect to the center of mass (c.m.). The analytical CTOCD-DZ estimates are obtained summing conventional χ^p and χ^Δ evaluated at c.m. via formal annihilation of the diamagnetic current density term. Analogously, CTOCD-PZ predictions are given by conventional χ^d plus χ^Π by formal annihilation of paramagnetic current density contribution.[42−48]

The CTOCD-DZ1 estimates are obtained via numerical integration. They should coincide with the analytical CTOCD-DZ. If small discrepancies are found, they depend on the error in numerical integration. In fact, the overall agreement is excellent. If the wave functions were exact eigenstates of a

TABLE 2: Magnetic Susceptibility of *s*-Indacene (ppm cgs au/molecule)[a]

	xx	*yy*	*zz*	av	$\Delta\chi$
χ^{d}	−16 607.67	−10 092.84	−25 160.69	−17 287.07	−11 810.43
χ^{d} (LO)	−16 607.65	−10 092.83	−25 160.66	−17 287.05	−11 810.42
χ^{Δ}	−16 393.16	−9962.45	−25 023.31	−17 126.30	−11 845.51
χ^{p}	15 726.10	9256.30	24 345.29	16 442.56	11 854.10
χ^{p} (LO)	15 931.06	9375.37	24 474.60	16 593.67	11 821.38
χ^{p}	15 929.55	9376.47	24 477.16	16 594.39	11 824.15
$\chi^{d} + \chi^{p}$	−881.58	−836.55	−815.39	−844.51	43.67
$\chi^{\Delta} + \chi^{p}$	−667.06	−706.15	−678.01	−683.74	8.59
χ^{DZ1}	−667.06	−706.09	−678.00	−683.72	8.57
$\chi^{d} + \chi^{\Pi}$	−678.12	−716.37	−683.53	−692.67	13.72
χ^{DZ2}	−666.36	−705.57	−675.65	−682.53	10.31
χ^{PZ2}	−672.79	−712.14	−665.53	−683.49	26.93
$\chi^{d} + \chi^{p}$ (LO)	−676.59	−717.46	−686.07	−693.37	10.96

[a] The origin is in the center of mass (c.m.). To obtain magnetic susceptibilities in cgs emu mol^{-1}, the numbers in the table are to be multiplied by $a_0^3 N = 8.923\,887\,8 \times 10^{-2}$; further conversion to SI units is obtained by 1 JT = 0.1 cgs emu.

model electronic Hamiltonian, satisfying hypervirial conditions,[49] the χ^{Δ} (from the CTOCD-DZ calculation) and the χ^{Π} contributions (from the CTOCD-PZ calculation) would be equal to the exact χ^{d} and χ^{p}, respectively, of the CO approach. In actual numerical studies, the closeness of these estimates gives a measure of the deviations from the Hartree−Fock limit. In fact, the last seven rows in Table 2 yield the criterion of quality that we were looking for.

Because of well-known shortcomings, the total CO results, that is, $\chi^{d}_{\alpha\beta} + \chi^{p}_{\alpha\beta}$, are slowly convergent and less accurate than corresponding CTOCD and LO predictions, which are quite close to one another. Actually, the differences among the estimates for tensor components and average magnetic susceptibility reported in the last six rows of Table 2 are approximately 2%. Therefore, it can be reasonably argued that these predictions are of near-Hartree−Fock quality and can be used for a reasonable assessment of aromaticity of *s*-indacene in connection with its magnetic properties.

It can be observed in Table 2 that the paramagnetic χ^{p}_{zz} contribution to magnetic susceptibility is very large but smaller than χ^{d}_{zz}. As a result, the total out-of-plane component is diamagnetic. Its numerical value is close to those of the in-plane components, so the anisotropy is fairly small, approximately 10 ppm. Small computational errors in numerical integration probably affect theoretical predictions of χ_{zz} and $\Delta\chi$ at the CTOCD-PZ2 level of accuracy; compare for the deviations of these values from those given by DZ, PZ, DZ2, and LO methods in Table 2. We could not reduce the discrepancies by enlarging the integration grids.

In any event, the other theoretical results for $\Delta\chi = \chi_{zz} - (1/2)(\chi_{xx} + \chi_{yy})$ are consistent and indicate that *s*-indacene can be classified as a nonaromatic molecule, because enhanced magnetic anisotropy is the epitome of aromaticity. In fact, the experimental $\Delta\chi$ of benzene is 669.1 ± 1 (cgs) ppm au.[50]

Theoretical nuclear magnetic shielding results for C5, a carbon atom belonging to the central six-membered ring, see Figure 1, are displayed in Table 3, which serves to establish the overall quality of different approximations to this molecular property. Table 3 is analogous to Table 2, and the symbols have similar meaning, that is, σ^{d} and σ^{p} denote diamagnetic and paramagnetic contributions, respectively. The origin of the gauge is either the center of mass or the nucleus in question. In exact Hartree−Fock calculations, corresponding to complete basis set, the sums $\sigma^{d}_{\alpha\beta} + \sigma^{p}_{\alpha\beta}$ evaluated at different origins via gaugeless basis sets would be the same. In this ideal case, they would also be identical to CTOCD-DZ, CTOCD-PZ, and LO values, which are origin-independent also for truncated basis sets.

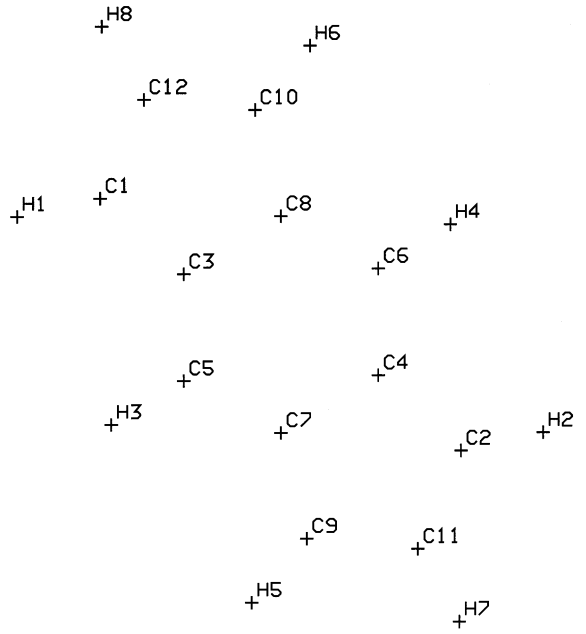

Figure 1. Numbering of atoms in the *s*-indacene molecule.

TABLE 3: Nuclear Magnetic Shielding of Carbon C5 in *s*-Indacene (ppm)[a]

	xx	*yy*	*zz*	*xy*	av	$\Delta\sigma$
C5						
σ^{d} (C5)	493.04	458.50	659.42	32.12	536.99	183.65
σ^{d} (c.m.)	459.91	368.95	536.74	89.10	455.20	122.31
σ^{d} (LO)	459.68	368.94	535.71	88.62	454.78	121.40
σ^{Δ}	482.28	448.14	649.64	31.76	526.68	184.43
σ^{p} (C5)	−551.34	−443.52	−494.15	−45.55	−496.34	3.27
σ^{p} (c.m.)	−518.85	−355.35	−372.01	−101.43	−415.40	65.09
σ^{p} (LO)	−521.89	−357.00	−372.63	−102.53	−417.17	66.82
σ^{Π}	−562.17	−452.29	−499.09	−46.09	−504.52	8.14
$\sigma^{d} + \sigma^{p}$ (C5)	−58.30	14.99	165.27	−13.42	40.65	186.93
$\sigma^{d} + \sigma^{p}$ (c.m.)	−58.94	13.60	164.73	−12.33	39.79	187.40
$\sigma^{\Delta} + \sigma^{p}$	−69.06	4.62	155.48	−13.79	30.35	187.70
σ^{DZ1}	−69.08	4.62	155.48	−13.79	30.34	187.71
$\sigma^{d} + \sigma^{\Pi}$	−69.14	6.21	160.33	−13.96	32.47	191.79
σ^{DZ2}	−62.01	11.63	162.68	−13.74	37.43	187.87
σ^{PZ2}	−62.43	11.41	162.27	−13.80	37.08	187.78
$\sigma^{d} + \sigma^{p}$ (LO)	−62.21	11.94	163.08	−13.91	37.61	188.22

[a] The origin is specified by the entry within parentheses, that is, center of mass (c.m.) and nucleus (C5). The LO results were obtained with the c.m. origin.

By inspection of Table 3, it is observed that the last three rows are virtually identical. The conclusion is that these predictions are of near-Hartree−Fock quality. Thus, only an

TABLE 4: Nuclear Magnetic Shielding of Carbon in *s*-Indacene (ppm)

	xx	*yy*	*zz*	*xy*	av	$\Delta\sigma$
			C1			
σ^{DZ2}	−73.57	39.38	146.32	33.95	37.38	163.42
σ^{PZ2}	−74.06	39.32	145.83	34.04	37.03	163.20
$\sigma^{d} + \sigma^{p}$ (LO)	−73.66	40.00	146.42	34.00	37.59	163.25
			C3			
σ^{DZ2}	−28.27	46.89	141.30	1.11	53.31	131.98
σ^{PZ2}	−28.50	46.79	140.85	1.11	53.05	131.70
$\sigma^{d} + \sigma^{p}$ (LO)	−28.42	47.34	141.29	0.99	53.41	131.83
			C7			
σ^{DZ2}	−24.26	35.85	147.75	−23.56	53.11	141.96
σ^{PZ2}	−24.52	35.73	147.32	−23.60	52.84	141.72
$\sigma^{d} + \sigma^{p}$ (LO)	−24.20	36.12	147.79	−23.75	53.24	141.82
			C9			
σ^{DZ2}	−39.28	−8.61	142.48	−30.47	31.53	166.43
σ^{PZ2}	−39.65	−8.91	142.01	−30.52	31.15	166.29
$\sigma^{d} + \sigma^{p}$ (LO)	−39.14	−8.48	142.66	−30.61	31.68	166.47
			C11			
σ^{DZ2}	0.46	27.41	147.15	40.51	58.34	133.21
σ^{PZ2}	0.19	27.30	146.61	40.57	58.03	132.86
$\sigma^{d} + \sigma^{p}$ (LO)	0.66	27.55	147.17	40.77	58.46	133.07

TABLE 5: Nuclear Magnetic Shielding of Hydrogen H3 in *s*-Indacene (ppm)[a]

	xx	*yy*	*zz*	*xy*	av	$\Delta\sigma$
H3						
σ^{d} (H3)	196.49	242.29	387.57	−43.08	275.45	168.18
σ^{d} (c.m.)	100.77	−24.52	25.03	118.44	33.76	−13.09
σ^{d} (LO)	101.87	−20.58	30.45	115.81	37.24	−10.20
σ^{Δ}	191.32	236.61	383.21	−42.63	270.38	169.24
σ^{p} (H3)	−170.97	−212.24	−360.12	40.56	−247.78	−168.51
σ^{p} (c.m.)	−77.85	47.24	−4.46	−116.58	−11.69	10.84
σ^{p} (LO)	−78.36	48.07	−4.34	−117.81	−11.54	10.80
σ^{Π}	−173.46	−215.24	−362.41	41.18	−250.37	−168.06
$\sigma^{d} + \sigma^{p}$ (H3)	25.51	30.05	27.45	−2.52	27.67	−0.33
$\sigma^{d} + \sigma^{p}$ (c.m.)	22.92	22.72	20.57	1.86	22.07	−2.25
$\sigma^{\Delta} + \sigma^{p}$	20.34	24.37	23.09	−2.07	22.60	0.73
σ^{DZ1}	20.34	24.37	23.09	−2.07	22.60	0.73
$\sigma^{d} + \sigma^{\Pi}$	23.02	27.06	25.16	−1.89	25.08	0.12
σ^{DZ2}	23.02	26.99	25.67	−2.02	25.23	0.67
σ^{PZ2}	23.39	27.41	25.90	−2.02	25.57	0.50
$\sigma^{d} + \sigma^{p}$ (LO)	23.51	27.48	26.10	−2.00	25.70	0.60

[a] The origin is specified by the entry within parentheses, that is, center of mass (c.m.) and nucleus (H3). The LO results were obtained for the c.m. origin.

analogous set of data is reported in Table 4 for other carbon nuclei, C1, C3, C7, and C11. A common trend emerging from theoretical calculations is that (i) the perpendicular shielding component is invariably larger than the in-plane components, (ii) its magnitude is larger for carbon nuclei within the six-membered ring, C5 and C6, bonded to hydrogen atoms H3 and H4, respectively, see Figure 1, (iii) for carbon atoms C3 and C7 belonging to two rings and C1 and C11 entering five-membered rings, the perpendicular component is ∼15−20 ppm smaller than that of C5. However, a rationalization of the observed carbon chemical shift in terms of ring currents does not seem viable, in accordance with previous findings.[51]

On the other hand, theoretical predictions for proton magnetic shielding tensor components are very important to analyze the aromaticity−antiaromaticity dilemma of *s*-indacene. A criterion of quality of the present study is obtained from Table 5, in which detailed information for hydrogen H3, see Figure 1, is available. The symbols are analogous to those introduced in Table 3.

The sums $\sigma^{d}_{\alpha\beta} + \sigma^{p}_{\alpha\beta}$ evaluated at different origins via gaugeless basis sets CO approaches are quite different, denoting slow convergence of the conventional procedure. The great advantages of the gauge-invariant CTOCD procedures are evident. In fact, the numerical predictions for tensor components and average values appearing in the last three rows are the same to three significant figures. It can be concluded that the DZ2, PZ2, and LO results are close to the Hartree−Fock limit.

TABLE 6: Nuclear Magnetic Shielding of Hydrogen in *s*-Indacene (ppm)

	xx	*yy*	*zz*	*xy*	av	$\Delta\sigma$
			H1			
σ^{DZ2}	22.81	27.12	26.88	0.66	25.61	1.91
σ^{PZ2}	23.19	27.51	27.13	0.68	25.94	1.78
$\sigma^{d} + \sigma^{p}$ (LO)	23.33	27.65	27.42	0.64	26.13	1.93
			H5			
σ^{DZ2}	24.02	25.62	26.78	−1.59	25.47	1.95
σ^{PZ2}	24.39	26.07	27.03	−1.55	25.83	1.80
$\sigma^{d} + \sigma^{p}$ (LO)	24.54	26.19	27.31	−1.56	26.01	1.95
			H7			
σ^{DZ2}	25.50	27.16	26.66	0.32	26.44	0.33
σ^{PZ2}	25.86	27.59	26.89	0.29	26.78	0.17
$\sigma^{d} + \sigma^{p}$ (LO)	26.07	27.70	27.16	0.33	26.97	0.27

Comparison with calculated values for hydrogen in benzene[52] is illuminating. In both molecules, the average of in-plane components, $(^1/_2)(\sigma^{H}_{xx} + \sigma^{H}_{yy})$, is ∼26 ppm, a typical result for planar conjugated hydrocarbons. In fact, the estimations are very close to one another, that is, 25.96 ppm in benzene, see Table 6 of ref 52, compared with 25.50 ppm in Table 5, predicted in the present calculations for *s*-indacene.

This suggests that, in the proximity of the proton in question, the electron flow induced by a uniform magnetic field along any direction parallel to the molecular plane has similar features. To right angles from the σ_h plane, this flow gives rise to comparable effects on magnetic shielding at the nucleus of hydrogens attached to benzene and to the central ring of *s*-indacene.

On the other hand, the out-of-plane component of proton shielding, $\sigma^{H3}_{zz} = 26.10$, is ∼5.45 ppm larger than that of benzene, 20.65 ppm, from Table 6 of ref 52. Thus theoretical average proton shieldings, 24.2 and 25.7 ppm, respectively, in benzene and *s*-indacene, are essentially biased by the ring currents induced by a magnetic field perpendicular to the molecular plane. According to the ring-current model[2,3] the high value of σ^{H3}_{zz} is indicative of a paramagnetic regime of currents induced by a magnetic field perpendicular to the molecular plane. As recalled previously, these currents cause upfield (downfield) chemical shift outside (inside) of the ring.

This hypothesis is confirmed by the high values of the perpendicular shielding component for hydrogens H1, H5, and H7 attached to the five-membered rings, see Table 6, for which only the near-Hartree−Fock predictions from DZ2, PZ2, and LO procedures were shown.

4. The Electron Current Density in *s*-Indacene

To ensure the certainty of the interpretation of *s*-indacene as a paratropic molecule, graphical representations of current density field were obtained by means of the CTOCD-DZ approach. As a matter of fact, it remains to be seen whether upfield proton shifts typical of this system are due to σ or π electron circulations. The plots of current density vector field, Figures 2−4, are very helpful to understand the phenomenology.

It can be observed from the streamline map on the top of Figure 2 that the π electrons sustain a delocalized anticlockwise circulation (assuming that the magnetic field points outward) all over the molecular perimeter, which can unequivocally be referred to as a paramagnetic ring current. Three paramagnetic

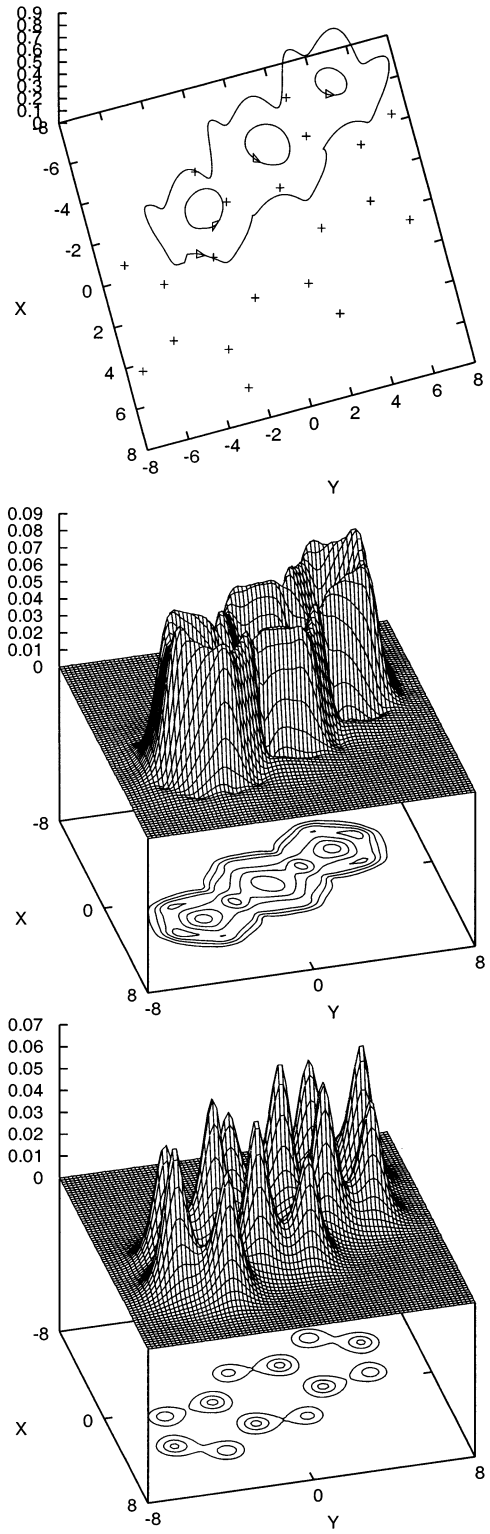

Figure 2. The spatial ring-current model for *s*-indacene: from top to bottom, streamlines of the paramagnetic π contribution to the current density vector field induced in the region of maximum π electron density by a magnetic field of unit magnitude at right angles to the molecular plane (the position of carbon and hydrogen nuclei is marked with a cross); 3D-perspective representations of $|\mathbf{J}|$, the modulus of the current density, and of ρ, the unperturbed π charge density (in au). The plots display a perspective view at points in a plane parallel to the plane of the molecule, displaced from it by 0.8 bohr. Corresponding contour maps are shown with values 0.01 k for $k = 0, 1, 2, ...$

vortices are found inside this external circuit, flowing about the center of five-membered and central carbon rings.

The leapfrog effect, due to a paramagnetic component parallel to the perturbing magnetic field,[53,54] is clearly visible. The nature of *delocalized ring current* of the external π-flow encompassing the molecule is explicitly established by comparison between the plots for $|\mathbf{J}|$ and ρ, the modulus of the current density field and the charge density, respectively. The latter contains much sharper peaks in the vicinity of each carbon atom, as observed in the 3D-perspective representation and in the contour maps, whereas $|\mathbf{J}|$ is more uniform over the peripheral carbon atoms.

Because the current density is written as $\mathbf{J} = \rho\mathbf{v}$, it can be argued that $\mathbf{v}$, the local average velocity, is higher in the interatomic regions than in the vicinity of the nuclei.[54] Quite remarkably, the intensity $|\mathbf{J}|$ of the paramagnetic flow in *s*-indacene has magnitude comparable with that of the diamagnetic ring current in benzene.[54]

Analogous plots for the total current sustained by σ and π electrons are shown in Figure 3. The striking feature is that the σ flow is more intense than that of π current, so the circulation in the tail regions of the molecular domain is diamagnetic. Only the paramagnetic vortices in the center of the carbon rings are still present in Figure 3.

The integral curves for the trajectories of the $\mathbf{J}$ vector on a plane parallel to that of the molecule at a distance of 0.8 bohr, corresponding to the perspective representations of Figures 2 and 3, are shown in Figure 4. The C_{2h} point group of the isolated molecule describes also the symmetry of the current density field. The topology of the flow is very complicated, and only curves that convey fundamental information are retained in the plot.

The paramagnetic ring currents are easy to detect in the streamline map on top of Figure 4. They surround completely the three vortices observable in Figure 2. They are separated by the typical phase portraits of saddle points between them.[2] The map suggests that they arise from bifurcation of a paramagnetic stagnation line.

On the bottom of the figure, it can be seen that the paramagnetic π ring current is partially overwhelmed by more intense σ diamagnetic flow. In any event, the paramagnetic vortices flowing around the center of the rings are maintained. This pattern is very interesting. It shows that the magnetic properties of *s*-indacene are typical of a system in which a peculiar interplay of σ and π currents determines a fairly unique response for unsaturated cyclic molecules. We believe that the residual paramagnetic ring currents would mainly determine also the magnetic shielding of a virtual probe in the center of pentagonal and hexagonal rings of *s*-indacene, that is, the large positive NICS values estimated in ref 32.

Two foci are found in Figure 4 at the opposite ends of the molecule. The continuity constraint is not violated in these singular points, which are connected by unique perpendicular current lines.

5. Paratropicity of *s*-Indacene via the Steiner−Fowler Approach

As outlined by Steiner and Fowler,[8,9] the distributed origin approach to first-order induced current density yields a simple interpretation of diatropicity and paratropicity of π currents through powerful group-theoretical criteria. In the ipsocentric[8,9] coupled Hartree−Fock CTOCD-DZ formulation,[45,46] the total current can be partitioned into orbital contributions made up of paramagnetic and diamagnetic terms. Within the DZ procedure, both terms are defined as sums over all possible transitions from the occupied to the virtual orbital space.

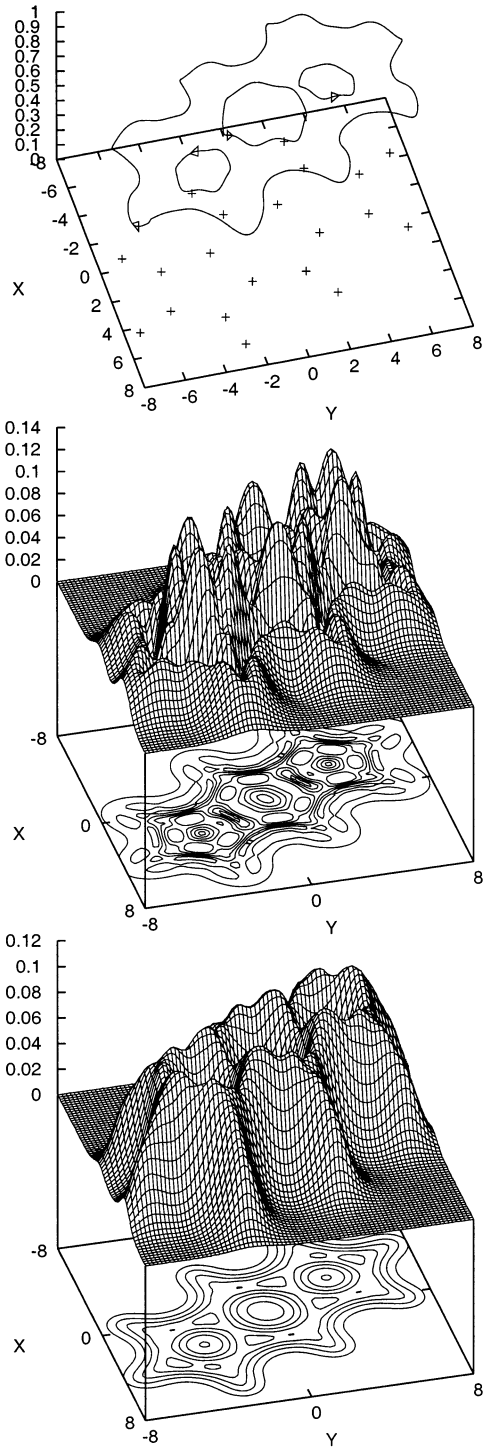

Figure 3. The spatial ring-current model for *s*-indacene: from top to bottom, streamlines of the total current density vector field induced in the region of maximum π electron density. The conventions are the same as in Figure 2. Contour maps are shown with values 0.02 k for $k = 0, 1, 2, ...$

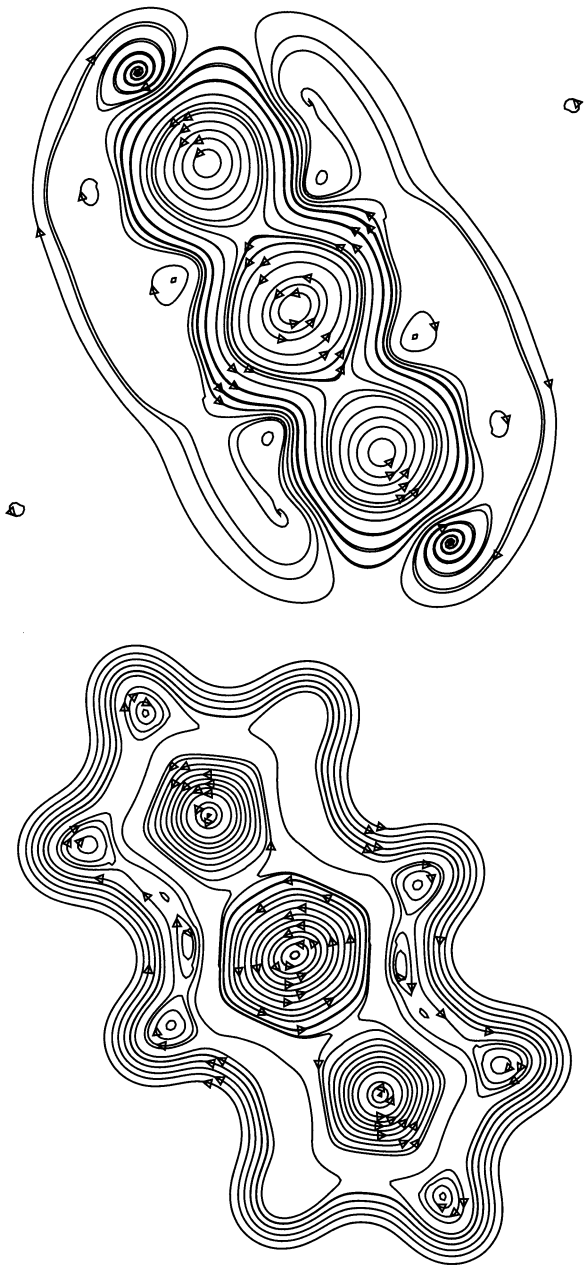

Figure 4. The integral trajectories of the **J** flux at 0.8 bohr above the molecular plane of *s*-indacene. The trajectories for the π contributions (total currents) are shown on the top (on the bottom) of the figure.

The diamagnetic orbital current density, $\mathbf{j}_i^{(d)}$, involves a sum over all virtual orbitals, ϕ_m, with energy, ϵ_m, of *translational* transition moments of the form $\langle\phi_m|p_\perp|\phi_i\rangle/(\epsilon_m - \epsilon_i)$, where ϕ_i is the occupied orbital with energy ϵ_i and $p_\perp$ denotes the components of the electronic linear momentum in the plane perpendicular to the applied magnetic field.

Analogously, the paramagnetic orbital current density, $\mathbf{j}_i^{(p)}$, involves a sum over all virtual orbitals of *rotational* transition moments of the form $\langle\phi_m|l_{||}|\phi_i\rangle/(\epsilon_m - \epsilon_i)$, where $l_{||}$ is the component of the electronic angular momentum operator parallel to the applied magnetic field. According to this scheme, it is evident that the diamagnetic and paramagnetic character of the total induced current density can be predicted in terms of the accessibility of virtual orbitals via translational and rotational transitions.

Because each transition depends on the inverse of virtual-occupied orbital energy differences, contributions by frontier orbital currents are expected to be dominant. Symmetry arguments can be invoked to determine whether a transition contributes at all to the current density.

Let G be the point group of the molecule and $\Gamma(T_\perp)$, $\Gamma(R_{||})$, $\Gamma(\phi_i)$, and $\Gamma(\phi_m)$ the irreducible representations of G for translations at right angles to the field, rotations around the field direction, the occupied orbital ϕ_i, and the virtual orbital ϕ_m (with similar nodal structure), respectively. According to the Wigner−

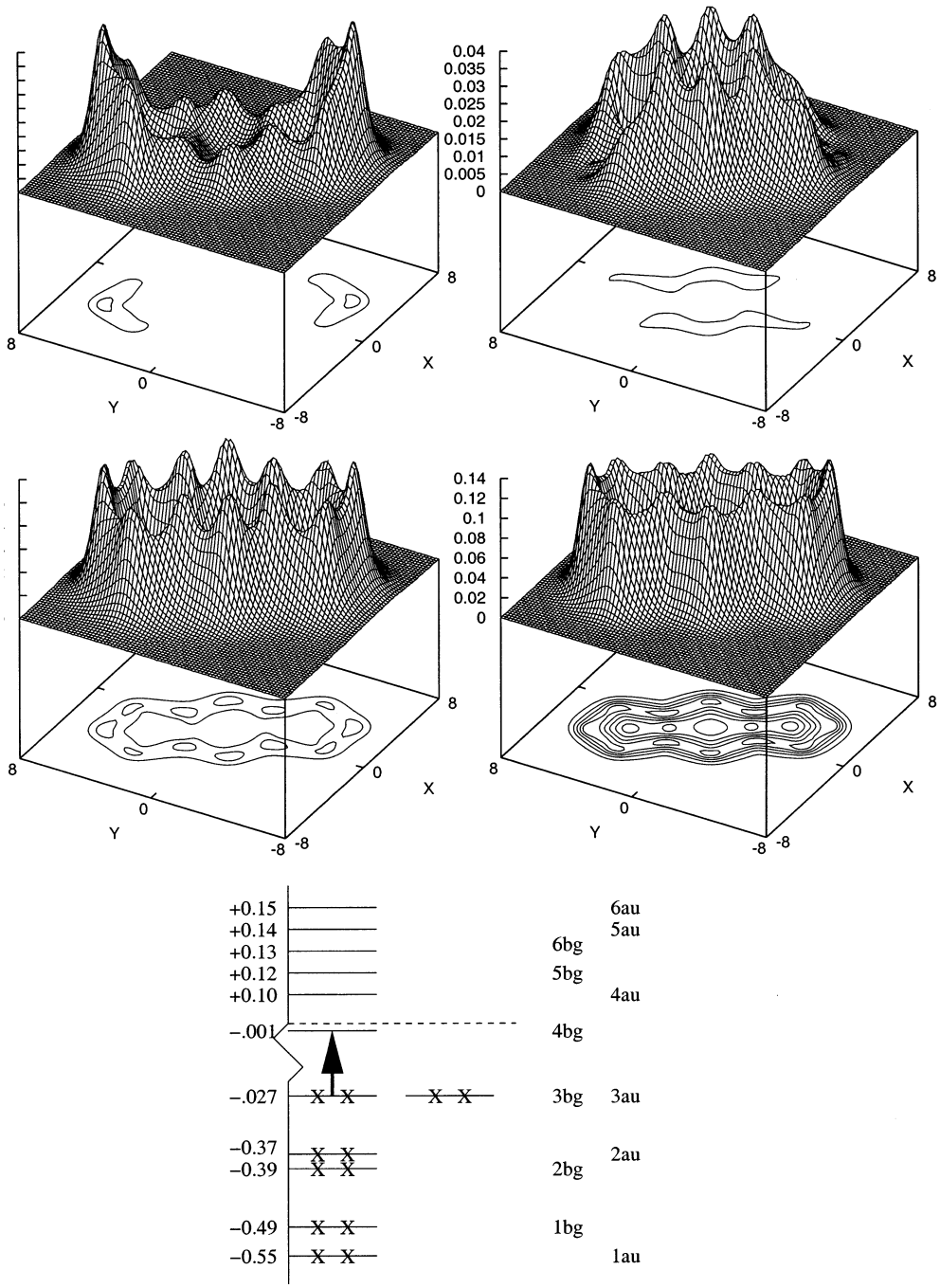

Figure 5. From left to right and top to bottom, modulus of the current density induced in the $2a_u$ and $3a_u$ orbitals, total $2a_u + 3a_u$, $3b_g$ orbital, and the orbital energies of the π electrons. The arrow indicates the excitation, which mainly determines the paramagnetic electron flow.

Eckhart theorem,[55] the $\phi_i \rightarrow \phi_m$ transition gives a nonvanishing contribution to the total diamagnetic (paramagnetic) current density if $\Gamma(\phi_i)\otimes\Gamma(T_\perp)\otimes\Gamma(\phi_m)(\Gamma(\phi_i)\otimes\Gamma(R_\parallel)\otimes\Gamma(\phi_m))$ contains the totally symmetric irreducible representation Γ_0.

Applying these simple and effective symmetry criteria, Steiner and Fowler[8,9] showed that magnetic response of planar conjugated molecules is always dominated by a few electrons occupying high-lying π orbitals. Typical diamagnetic systems (e.g., benzene, naphthalene) carrying strong diatropic π ring currents were shown to obey a 4d rule: only four electrons essentially bias the overall magnetic response. They occupy the two highest-lying orbitals, which undergo only translational transitions allowed by selection rules.

On the other hand, typical paramagnetic π networks carrying strong paratropic ring currents (e.g., cyclobutadiene, cyclooctatriene) obey a 2p rule: magnetic response is dominated by two electrons in the highest occupied molecular orbital (HOMO), which gives rise to rotational transitions only. Interesting pictorial interpretations were also given for systems that exhibit coexisting diatropic and paratropic currents, such as the 2p + 4d pyracylene system.[8]

The *s*-indacene molecule has a C_{2h} ground-state geometry. Accordingly, π orbitals transform as A_u and B_g irreducible representations. If the uniform external magnetic field is taken perpendicular to the molecular plane, then the translations at right angles to the perturbation transform as B_u and rotations around the field direction are totally symmetric. Therefore, $A_u \rightarrow A_u$ and $B_g \rightarrow B_g$ transitions are rotationally allowed, leading to paramagnetic orbital contributions. $A_u \rightarrow B_g$ and $B_g \rightarrow A_u$

transitions are translationally allowed, leading to diamagnetic orbital contributions.

The analysis of the π orbital energy-level diagram, Figure 5, does not lend itself to immediate conclusions. It can be noticed from the start that the minimal (π,π*) space is large enough to allow both translational and rotational transitions weighted by comparable energy gaps from each occupied orbital. The A_u HOMO and the B_g HOMO-1 are nearly degenerate. The lowest unoccupied molecular orbital (LUMO) has B_g symmetry. It follows that the two dominant transitions, namely, the HOMO−LUMO $A_u \rightarrow B_g$ and (HOMO-1)−LUMO $B_g \rightarrow B_g$, have opposite effects. Group theory and considerations of orbital energies are not sufficient to characterize the magnetic response of the system a priori. A similar situation is found by analyzing (HOMO-2)−LUMO and (HOMO-3)−LUMO transitions.

The CTOCD-DZ plots of the orbital currents provide a further piece of information via some pictorial MO analysis. The ab initio calculation demonstrates that the total π current is dominated by six electrons occupying the $3a_u$ HOMO, the nearly degenerate $3b_g$ HOMO-1, and the $2a_u$ HOMO-2. Figure 5 shows the plots of the modulus of the dominant orbital current densities at 0.8 bohr above the molecular plane. They can be compared with corresponding maps for total π current density in Figure 2.

The paramagnetic circulation associated with two electrons in the $3b_g$ orbital is delocalized all over the molecular perimeter with almost uniform intensity, just like the total paramagnetic π current. Interestingly enough, the maximum intensity of the latter, ∼0.09 au, is smaller than that of the former, ∼0.14 au. This pattern can be easily explained on the grounds that the four-electron diamagnetic contributions of the $3a_u$ HOMO and $2a_u$ HOMO-2 orbital currents sum up to determine a diatropic circulation uniformly delocalized over the molecular skeleton with maximum modulus ≈ 0.06 au. Then the maximum modulus of the total paramagnetic current density is recovered by subtracting these values.

Pictorial orbital analysis provided by the CTOCD-DZ formulation of magnetic properties confirms the peculiarity of the *s*-indacene molecule. As in other planar polycyclic conjugated hydrocarbons, the electronic response to magnetic perturbation is dominated by a few electrons close to the molecular "Fermi level". According to the nomenclature introduced by Steiner and Fowler,[8,9] *s*-indacene can be classified as a 2p + 4d system.

The special character of its π cloud arises from the fact that the total π current is purely paramagnetic: diatropicity and paratropicity do not coexist in *s*-indacene, as they do in other 2p + 4d molecules such as pyracylene. The dominant paramagnetic circulation accounted for by a strong 2p transition, that is, a fingerprint of antiaromaticity according to magnetic criteria, is significantly quenched by a 4d diatropic response typical of an aromatic diamagnetic molecule. Therefore, the resulting paratropic pattern results from a superposition of two opposing driving mechanisms that seem to determine the mixed aromatic and antiaromatic character of *s*-indacene at a simple molecular orbital level.

6. Concluding Remarks

Near-Hartree−Fock calculations of magnetic properties and visualizations of the current density vector field demonstrate that a magnetic field perpendicular to the molecular plane of *s*-indacene induces strong delocalized paramagnetic ring currents within its π-electron cloud. The intensity of the π currents along the molecular carbon skeleton is comparable to that of the diamagnetic flow in benzene. Three juxtaposed paramagnetic vortices were found about the center of the hexagonal and pentagonal carbon rings.

The paramagnetic circulation is supposed to cause an upfield shift as large as ∼5.5 ppm with respect to benzene for the perpendicular shielding component of protons in the central ring. Nuclei of hydrogen atoms attached to the five-membered rings are also extra-shielded. In the peripheral regions of the molecular domain, the diamagnetic circulation of σ electrons overpowers the paramagnetic regime, which explains why the diagonal components and the average value of the magnetic susceptibility tensor are negative, denoting overall diamagnetism of the molecule. The anisotropy of the magnetic susceptibility is predicted to be quite small. This indicates that *s*-indacene is not aromatic on the basis of magnetic criteria.

Previous findings suggest that this system may be regarded as possessing mixed aromatic and antiaromatic properties.[32] The evidence arrived at in the present work by evaluating magnetic properties confirms the hypothesis and documents the exceptional features of *s*-indacene. Even if the molecule has not yet been synthesized and despite of the fact that no proof of its thermodynamic stability has been reported so far, the conceptual importance of this system cannot be overemphasized. It provides a remarkable model for a peculiar magnetic response. It exhibits mixed aromatic and antiaromatic properties and constitutes a prototype of "paratropic, but non-antiaromatic system". As such, it can serve to identify a limit behavior and to ideally separate classes of aromatic and antiaromatic molecules.

Acknowledgment. Financial support of the present research from the European research and training network "Molecular Properties and Materials (MOLPROP)", contract No. HPRN-CT-2000-00013, from the Italian MURST (Ministero dell'Università e della Ricerca Scientifica e Tecnologica) via 60% and 40% funds is gratefully acknowledged.

References and Notes

(1) Haley, M. M.; Pak, J. J.; Brand, S. C. **1999**, *201*, 81.
(2) Lazzeretti, P. Ring currents. *Progress in Nuclear Magnetic Resonance Spectroscopy*; Elsevier: Amsterdam, 2000; Vol. 36, p 1−88.
(3) Gomes, J. A. N. F.; Mallion, R. B. *Chem. Rev.* **2001**, *101*, 1349.
(4) Krygowski, T. M.; Cyranski, M. K.; Czarnocki, Z.; Häfelinger, G.; Katryzki, A. R. *Tetrahedron* **2000**, *56*, 1783.
(5) Cyranski, M. K.; Stepien, B. T.; Krygowski, T. M. *Tetrahedron* **2000**, *56*, 9663.
(6) Steiner, E.; Fowler, P. W. *Int. J. Quantum Chem.* **1996**, *60*, 609.
(7) Cernusak, I.; Fowler, P. W.; Steiner, E. *Mol. Phys.* **1997**, *91*, 401.
(8) Steiner, E.; Fowler, P. W. *J. Phys. Chem. A* **2001**, *105*, 9553.
(9) Steiner, E.; Fowler, P. W. *Chem. Commun.* **2001**, 2220.
(10) Steiner, E.; Fowler, P. W. *ChemPhysChem* **2002**, *3*, 114.
(11) Steiner, E.; Fowler, P. W.; Jenneskens, L. W. *Angew. Chem., Int. Ed.* **2001**, *40*, 362.
(12) Acocella, A.; Havenith, R. W. A.; Steiner, E.; Fowler, P. W.; Jenneskens, L. W. *Chem. Phys. Lett.* **2002**, *363*, 64.
(13) Mitchell, R. H. *Chem. Rev.* **2001**, *101*, 1301.
(14) von Ragué Schleyer, P. *Chem. Rev.* **2001**, *101*, 1115.
(15) Minkin, V. I.; Glukhovtsev, M. N.; Simkin, B. Y. *Aromaticity and Antiaromaticity, Electronic and Structural Aspects*; John Wiley and Sons: New York, 1994.
(16) Mills, N. S.; Malandra, J. L.; Burns, E. E.; Green, A.; Gibbs, J.; Unruh, K. E.; Kadlecek, D. E.; Lowery, J. A. *J. Organomet. Chem.* **1998**, *62*, 9318.
(17) Mills, N. S.; Burns, E. E.; Hodges, J.; Gibbs, J.; Esparza, E.; Malandra, J. L.; Koch, J. *J. Organomet. Chem.* **1998**, *63*, 3017.
(18) Alkorta, I.; Rozas, I.; Elguero, J. *Tetrahedron* **2001**, *57*, 6043.
(19) Berthier, G.; Mayot, M.; Pullman, B. *J. Phys. Radium* **1951**, *12*, 717.
(20) London, F. *J. Phys. Radium*. **1937**, *8* (7ème Série), 397.
(21) Salem, L. *The Molecular Orbital Theory of Conjugated Systems*; W. A. Benjamin Inc.: New York, 1966.

(22) Pople, J. A.; Untch, K. G. *J. Am. Chem. Soc*. **1966**, *88*, 4811.
(23) Sondheimer, F. *Pure Appl. Chem*. **1963**, *7* (Suppl. 2), 363.
(24) Hafner, K.; Hafner, K. H.; König, C.; Kreuder, M.; Ploss, G.; Schulz, G.; Sturm, E.; Vöpel, K. H. *Angew. Chem., Int. Ed. Engl*. **1963**, *2*, 123.
(25) Hafner, K.; Stowasser, B.; Krimmer, H.-P.; Fischer, S.; Böhm, M. C.; Lindner, J. H. *Angew. Chem., Int. Ed. Engl*. **1986**, *25*, 630.
(26) Dunitz, J. D.; Krüger, C.; Irngartinger, H.; Maverick, E. F.; Yang, Y.; Nixdorf, M. *Angew. Chem., Int. Ed. Engl*. **1988**, *27*, 387.
(27) Heilbronner, E.; Yang, Z.-Z. *Angew. Chem., Int. Ed. Engl*. **1987**, *26*, 360.
(28) Heilbronner, E. *J. Chem. Educ*. **1989**, *66*, 471.
(29) Nakajima, T.; Saijo, T.; Yamaguchi, H. *Tetrahedron* **1964**, *20*, 2119.
(30) Gellini, C.; Cardini, G.; Salvi, P. R.; Marconi, G.; Hafner, K. *J. Phys. Chem*. **1993**, *97*, 1286.
(31) Hertwig, R. H.; Holthausen, M. C.; Koch, W.; Maksić, Z. B. *Angew. Chem., Int. Ed. Engl*. **1994**, *33*, 1192.
(32) Nendel, M.; Goldfuss, B.; Houk, K. N.; Hafner, K. *J. Mol. Struct. (THEOCHEM)* **1999**, *461*−*462*, 23.
(33) Hertwig, R. H.; Holthausen, M. C.; Koch, W.; Maksić, Z. B. *Int. J. Quantum Chem*. **1995**, *54*, 147.
(34) von Ragué Schleyer, P.; Maerker, C.; Dransfeld, A.; Jiao, H.; van Eikema Hommes, N. J. R. *J. Am. Chem. Soc*. **1996**, *118*, 6317.
(35) Jusélius, J.; Sundholm, D. *Phys. Chem. Chem. Phys*. **1999**, *1*, 3429.
(36) Juselus, J.; Sundholm, D. *Phys. Chem. Chem. Phys*. **2001**, *3*, 2433.
(37) Frisch, M. J.; Trucks, G. W.; Schlegel, H. B.; Gill, P. M. W.; Johnson, B. G.; Robb, M. A.; Cheeseman, J. R.; Keith, T.; Petersson, G. A.; Montgomery, J. A.; Raghavachari, K.; Al-Laham, M. A.; Zakrzewski, V. G.; Ortiz, J. V.; Foresman, J. B.; Cioslowski, J.; Stefanov, B. B.; Nanayakkara, A.; Challacombe, M.; Peng, C. Y.; Ayala, P. Y.; Chen, W.; Wong, M. W.; Andres, J. L.; Replogle, E. S.; Gomperts, R.; Martin, R. L.; Fox, D. J.; Binkley, J. S.; Defrees, D. J.; Baker, J.; Stewart, J. P.; Head-Gordon, M.; Gonzalez, C.; Pople, J. A. *Gaussian 94*, revision B.3; Gaussian, Inc.: Pittsburgh, PA, 1995.
(38) Lazzeretti, P.; Malagoli, M.; Zanasi, R. *Technical report on project "sistemi informatici e calcolo parallelo"*; Research Report 1/67; CNR: Rome, 1991.
(39) van Duijneveldt, F. B. *Gaussian basis sets for the atoms H*−*Ne for use in molecular calculations*; Research Report RJ 945; IBM: Yorktown Heights, NY, 1971.
(40) Helgaker, T.; Jensen, H. J. A.; Jørgensen, P.; Olsen, J.; Ruud, K.; Ågren, H.; Auer, A. A.; Andersen, T.; Bak, K. L.; Bakken, V.; Christiansen, O.; Coriani, S.; Dahle, P.; Dalskov, E. K.; Enevoldsen, T.; Fernandez, B.; Hättig, C.; Hald, K.; Halkier, A.; Heiberg, H.; Hettema, H.; Jonsson, D.; Kirpekar, S.; Kobayashi, R.; Koch, H.; Mikkelsen, K. V.; Norman, P.; Packer, M. J.; Pedersen, T. B.; Ruden, T. A.; Sanchez, A.; Saue, T.; Sauer, S. P. A.; Schimmelpfenning, B.; Sylvester-Hvid, K. O.; Taylor, P. R.; Vahtras, O. *Dalton, An electronic structure program*, release 1.2; Dalton: 2001.
(41) Hansen, A. E.; Bouman, T. D. *J. Chem. Phys*. **1985**, *82*, 5035.
(42) Lazzeretti, P.; Malagoli, M.; Zanasi, R. *J. Chem. Phys*. **1995**, *102*, 9619.
(43) Lazzeretti, P.; Zanasi, R. *Int. J. Quantum Chem*. **1996**, *60*, 249.
(44) Zanasi, R. *J. Chem. Phys*. **1996**, *105*, 1460.
(45) Lazzeretti, P.; Malagoli, M.; Zanasi, R. *Chem. Phys. Lett*. **1994**, *220*, 299.
(46) Coriani, S.; Lazzeretti, P.; Malagoli, M.; Zanasi, R. *Theor. Chim. Acta* **1994**, *89*, 181.
(47) Zanasi, R.; Lazzeretti, P.; Malagoli, M.; Piccinini, F. *J. Chem. Phys*. **1995**, *102*, 7150.
(48) Zanasi, R.; Lazzeretti, P.; Fowler, P. W. *Chem. Phys. Lett*. **1997**, *278*, 251.
(49) Epstein, S. T. *The Variation Method in Quantum Chemistry*; Academic Press: New York, 1974.
(50) Hoarau, J.; Lumbroso, N.; Pacault, A. C. R. *Acad. Sci. (Paris)* **1956**, *242*, 1702.
(51) Fleischer, U.; Kutzelnigg, W.; Lazzeretti, P.; Mühlenkamp, V. *J. Am. Chem. Soc*. **1994**, *116*, 5298.
(52) Ligabue, A.; Lazzeretti, P. *J. Chem. Phys*. **2002**, *116*, 964. EPAPS material available at http://www.aip.org/pubservs/epaps.html.
(53) Ligabue, A.; Soncini, A.; Lazzeretti, P. *J. Am. Chem. Soc*. **2002**, *124*, 2008.
(54) Ligabue, A.; Lazzeretti, P. *J. Chem. Phys*. **2002**, *116*, 964.
(55) McWeeny, R. *Symmetry*; Pergamon Press: Oxford, U.K., 1963.